16th World Conference on Earthquake Engineering, 16WCEE 2017

Santiago Chile, January 9th to 13th 2017

Paper N° 1263

Registration Code: S-E1463442016

SIMPLIFIED ANALYTICAL METHOD TO PREDICT THE FAILURE PATTERN OF INFILLED RC FRAMES

J. Martín Tempestti[(1)], A. Stavridis[(2)]

[(1)] *Structural Engineer, CIES Structural Engineering Consultancy, jimenaya@buffalo.edu*
[(2)] *Assistant Professor, Civil Structural and Environmental Engineering, University at Buffalo, astavrid@buffalo.edu*

Abstract

This paper presents a numerical study on the seismic performance of reinforced concrete (RC) frames with masonry infill walls. The study is based on an extensive parametric study using a detailed finite element model validated with laboratory tests. The model combines the discrete and smeared crack modeling approaches to capture the diffused flexural and dominant shear cracks in the RC members, the crushing and tensile splitting of the masonry units, as well as the mixed-mode fracture of the mortar joints. The study examines the influence of a number of geometric and design parameters on the seismic performance of these structures and proposes a simplified methodology to predict the failure pattern under in-plane seismic loads. The proposed methodology classifies the infilled frames based on the relative strength and stiffness of the frame and the infill. The results of this procedure have been used successfully to predict the response of experimentally tested infilled RC frames. The comparison of the predicted and experimentally observed responses indicates that the proposed methodology can predict the failure mechanism with sufficient accuracy.

Keywords: infilled reinforced concrete frames, in-plane lateral resistance, failure mechanism, parametric study.

1. Introduction

Masonry-infilled reinforced concrete (RC) frames have suffered catastrophic failures due to earthquakes across the world. The prediction of their seismic performance is a major challenge for practicing engineers who are tasked with the seismic assessment of these buildings. However, there is a lack of reliable, yet efficient, methods that can be used to accurately predict their performance due to the nonlinear behavior of the masonry panels and the bounding RC frames, which also interact under seismic forces. Guidelines can be found in ASCE 41 [1, 2]. However, these guidelines focus on individual members, are incomplete, and do not provide information on the peak strength and post-peak behavior of these structures or the failure mechanism.

A number of methods have been proposed to estimate important features of the seismic response of infilled RC frames. The most commonly used method utilizes diagonal struts to model the effect of infills [3]. The equivalent strut typically has the same thickness and material properties as the masonry panel, while the strut width is estimated with empirical formulas as it cannot be determined explicitly. As a result, a variety of implementations have been proposed typically based on case-specific data and lack general applicability. An alternative to the strut method is the limit analysis method in which the capacity is estimated once a failure mechanism is assumed [4, 5, 6]. However, in most cases, the failure pattern is not known *a priori*. Hence, the applicability of this method is quite limited as well.

The most accurate method currently available that can predict such features of the response, is the analysis using detailed finite elements (FE) [7, 8, 9] which can provide information on the failure pattern, as well as the force-vs.-displacement curve. The use of this method, however, is limited as it requires a considerable amount of effort to assemble and calibrate such models for actual structures while the computational effort required to run the analyses of actual size structures is also prohibitive [10].

This paper discusses a methodology that can predict the failure mechanism of infilled RC frames. The proposed methodology is based on the results of an extensive parametric study on the performance of RC frames with solid masonry infills, conducted using a detailed FE modeling scheme validated with experimental data [9]. The parametric study considers the effects of the frame geometry, vertical load, flexural and shear reinforcement, as well as the material properties of the infill. The results of the parametric study indicate that two indices can be used to classify the structures. The relative stiffness of the infill with respect to the stiffness of the surrounding frame controls the behavior of the infill and it can be used to classify the infill as strong or weak. Moreover, the ratio of the shear to the flexural capacity of the columns can determine whether the frame will behave in a ductile or non-ductile manner. In this study, criteria are proposed for the classification of the infill as strong or weak, and the frame as ductile or non-ductile. Consequently, the infilled frames can be classified in four categories each of which is associated with a distinct failure mechanism. The proposed methodology is validated with the FE models of the parametric study as well as the data from laboratory tests available in the literature.

2. Numerical Parametric Study

A parametric study is conducted to enhance the experimental database. The study uses the validated FE modeling scheme proposed by Stavridis and Shing [9] to further investigate the influence of a number of parameters on the structural response. Specimen M8 tested by Mehrabi et al. [6] and specimen CU1 that had solid infill [11] are used to validate the FE model and also provide references for the geometry, reinforcement detailing, vertical load, and material properties in the parametric study. The specimens are selected, due to the distinct designs and failure patterns. Specimen M8 incorporated a weak infill that developed significant sliding and crushing leading to a flexure-dominated ductile failure of the RC columns. Specimen CU1 represented 1920s construction in California and had a strong infill that developed a dominant shear crack that propagated through the column leading to a brittle, shear dominated failure of the RC columns. The behavior of these specimens has been successfully simulated with a modeling scheme for the RC members and the masonry panels illustrated in Fig.1. As shown in the figure the scheme combines the smeared and discrete crack approaches to capture the different failure modes of infilled frames, including the mixed-mode fracture of mortar joints, the crushing and cracking of the masonry, and the flexural and shear failure of RC members. Details about the constitutive models and calibration procedure can be found in [9]. Figures 2 and 3 present the experimental and numerical results for Specimen M8, [6] and CU1 [11] and demonstrate the capability of the model to capture the distinct failure mechanisms [11].

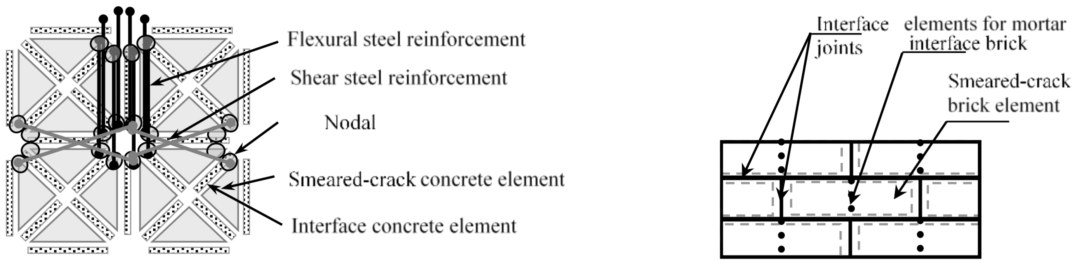

a. RC members b. masonry infill

Fig. 1 - Finite-element discretization schemes [11]

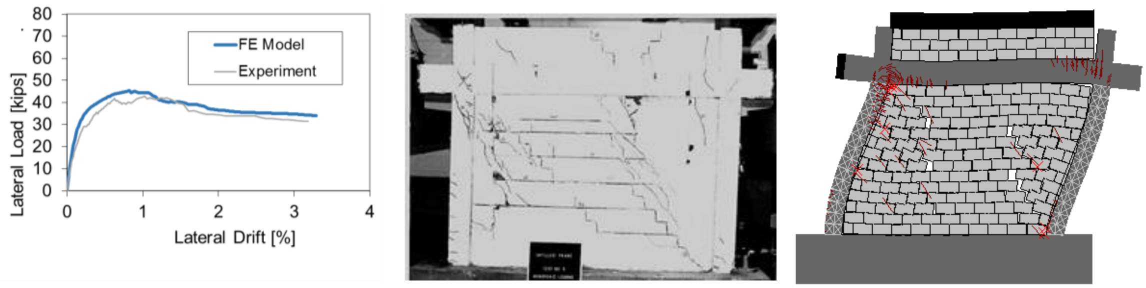

a. analytical and experimental force-displacement curve b. experimental failure pattern c. finite element model failure pattern at 0.8% drift

Fig. 2 - Comparison of experimental and numerical models for Specimen M8 [9, 6]

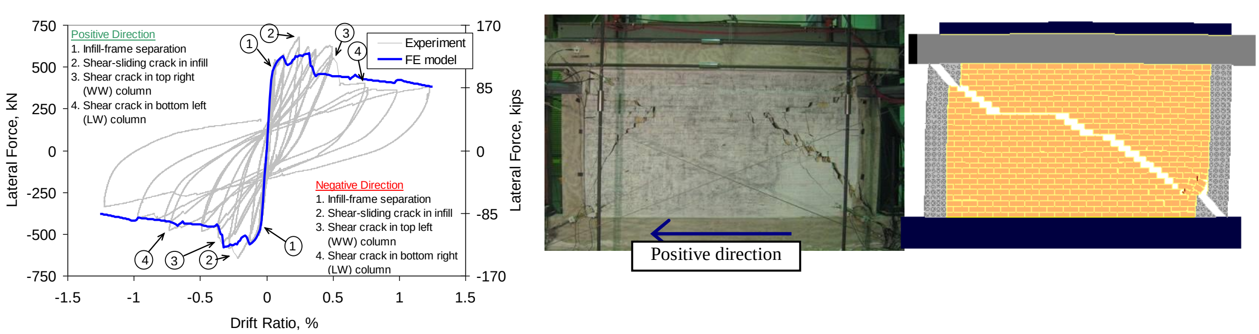

a. analytical and experimental force-displacement curve b. experimental failure pattern at 1% drift c. finite element model failure pattern at 1% drift

Fig. 3 - Comparison of experimental and numerical models for Specimen CU1 [9, 11]

Three base models are considered as reference models for the parametric study. All three reference models, have the same geometry and concrete material properties to limit the variables between the different models. The first model, identified as CU1, is based on the CU1 Specimen tested at the University of Colorado [12], the second reference model, CU1M8, combines the RC frame of CU1 with the infill found in Specimen M8 [6] which included hollow units, while the third reference model, CU1S, is also based on CU1 but includes four times the shear reinforcement as the stirrup spacing is reduced from 28 cm in CU1 to 7 cm.

Using the models of CU1, CU1M8 and CU1S as references, models for 53 cases were created by varying one design or geometric parameter with respect to one of the reference models at the time. The name for each frame includes an indication of the reference model used to generate and an ending indicating the variable being changed for the particular case, and numbers indicating the value of that parameter. Hence, 'F' indicates a change in the vertical load; 'AR' a change in the aspect ratio h_{inf}/L_{inf}; 'St' a change in the area of stirrups; 'D' different stirrup spacing; 'Ro' a variation in the longitudinal steel area, and 'C' a change in the column width. For example, model P1F40 is from the first set of models based on CU1 but has the vertical load changed to 178kN which is equivalent to 40kips [13]. The design details of the models considered are shown in Tables 1 and 2.

Table 1 – Design details of base models in parametric study

10	Vertical load	Infill aspect ratio (h_{inf}/L_{inf})	Total Stirrup area	Stirrup spacing	Column reinforcing ratio	Column size
	kN	-	cm^2	cm	%	cm
CU1	338	0.56	0.97	29.2	1%	28 x 28
CU1M8	338	0.56	0.97	29.2	1%	28 x 28
CU1S	338	0.56	0.97	7.3	1%	28 x 28

Table 2. Parametric study overview [14]

Parametric study set	Infill material properties	RC Frame material properties	Frame & infill dimensions	Parameter changed					
				Vertical load	Aspect ratio	Transverse steel	Transverse steel spacing	Longitudinal steel	Column width
1	CU1	CU1	CU1	X	X	X	X	X	
2	M8	CU1	CU1	X	X	X	X	X	
3	CU1	CU1S	CU1	X	X	X			X

3. Results of the Parametric Study

The results of the parametric study are used here to classify the infilled frames according to their behavior. First, the infill is classified as when it has a relatively small contribution to the overall strength it is referred to as 'weak infill'; while, in case it dominates the capacity it is referred to as 'strong infill'. The overall behavior is classified as brittle or ductile based on the failure pattern and the force-vs.-displacement relationship. The brittle behavior is typically associated with major shear cracks in the columns which develop as dominant sliding/diagonal cracks propagate in the infill, while the ductile behavior involves sliding or crushing in the infill and diffused minor shear cracks leading to plastic hinges in the columns.

3.1 Effect of Aspect Ratio

The infill walls of the reference models have an infill aspect ratio, h_{inf}/L_{inf}, of 0.56 based on the geometry of CU1. In the parametric study, the length of the infill is varied so that the aspect ratio changes between 2.63 and 0.38. Frames with longer infill walls, hence a smaller aspect ratio, have higher capacity to lateral loads, mainly because the cross section of the infill increases. This increases the area that resists the lateral force through cohesion. Moreover, the larger distance between the columns reduces the axial forces that develop to resist the overturning moment. This is particularly beneficial for the windward column whose shear capacity increases as the induced tension is reduced. The structures with longer infills and therefore larger infill cross section, also have higher stiffness which leads to lower drift at peak load. As the stiffness and strength increase however, the failure pattern is more brittle as it is dominated by shear cracks. On the contrary, the narrow walls with larger aspect ratios deform in a flexural manner, similar to the bare frame, and have rather low stiffness.

3.2 Effect of Infill Strength

The infill of CU1 included two wythes of solid clay bricks and had a prism strength of 23MPa. The infill of Specimen 8 tested by Mehrabi et al. [6] had hollow concrete units and a prism strength of 9.5MPa. The comparison of the performance of the corresponding frames from the CU1 and CU1M8 reference models indicates that structures with weaker and less stiff infills exhibit a more ductile behavior. This can be expected and it is attributed to the crushing and sliding of the weak infill. That limits its load carrying capacity and the forces transferred from the infill to the RC frame. Hence, the latter can deform more due to the reduced resistance provided by the infill. As a result, a longer part of the column is mobilized to accommodate the lateral drift. This reduces the shear demand on the columns leading to a flexure-dominated behavior for the RC frame.

3.3 Effect of Vertical Load

In all three sets of models, the applied vertical load is varied from 0kN to 533kN or 711kN. In general, a larger axial load increases the shear capacity of the infill frame. Hence, in all cases, the peak lateral resistance increases proportionally to the increase of the vertical load. However, it is important to note that this increase is limited by the compression capacity of the infill. This is evident when the load increases from 533kN to 711kN (P1F120 to P1F160 and P2F120 to P2F160). In this case there is no significant gain in the lateral strength of the infilled frame as the infill crushes under the combination of the vertical and lateral load.

In the cases of low vertical load, the lateral resistance is also not proportional to the applied vertical load. In the case of low lateral load, the dilation of the infill is resisted by the bounding frame. Hence, even in the absence of significant externally applied vertical load, a portion of the masonry infill dilates vertically as it slides along the bed joints and compressive stresses develop between the bounding frame and the infill [13]. This effect is minimized as the applied vertical load increases and dominates over the load induced due to the restrained dilation.

3.4 Effect of Shear Reinforcement

The shear reinforcement is increased both in terms of the size of the bars used, as well as the spacing. The results of the study indicate that the findings are similar in both cases, in that an increase in the shear reinforcement does not influence the initial stiffness and peak strength significantly. However, it has a noticeable effect on the failure mechanism of the columns, as well as the residual load capacity and the ductility of the structure. As the amount of shear reinforcement increases, either by increasing the stirrup size or by decreasing the stirrup spacing, the residual capacity increases and the behavior can change from brittle to ductile.

3.5 Effect of Longitudinal Reinforcement

The three base models have a longitudinal reinforcement ratio of 1%. In this study, this quantity is varied from 0.5% to 4% at base models CU1 and CU1M8. As discussed earlier, in case of a strong infill, the infill dominates the response and does not allow the lateral deformation of the surrounding columns which are subjected to high shear forces. Therefore, in this case the role of the flexural reinforcement is limited and its amount is not as important. The amount of longitudinal reinforcement impacts the flexural capacity which can affect the failure mode of the frame in the case of a weak infill. Hence, in this case, the increase of longitudinal reinforcement if not combined with the addition of shear reinforcement can cause the brittle failure of the frame.

3.6 Effect of Column Width

The column width is only changed in the set of models that used CU1S as a reference structure. In this reference structure the amount of shear reinforcement increases as the spacing is reduced to ¼ of the distance in CU1. In addition to this, the width of the columns is varied from 28cm to 20, 30, and 41cm in other models to influence the shear capacity more drastically than the flexural capacity. The results indicate that as the column width increases, the column capacity and the strength of the frame increase, as expected, and the failure mode of the RC columns changes from shear to flexure-dominated. In more detail, the frame with 20-cm wide columns, fails due major cracks shear failure in the columns, while the frame in which the columns are 41-cm wide, exhibits a flexure dominated failure mechanism as the increased column width increases its shear resistance.

4. Failure Mechanisms

4.1 Description of failure mechanisms

In all cases considered, damage initiates in the infill and then it propagates into the columns. Hence, the behavior of the infill should be considered first. As discussed earlier, the masonry infills can be characterized as strong or weak. In the case of a 'strong' infill, a dominant shear-sliding crack typically develops. This crack in most cases initiates near the top of the windward column and propagates through the infill to the bottom of the leeward column. In the case of a weak infill, shear sliding is observed along the joints throughout the infill, while crushing can be also observed near the columns.

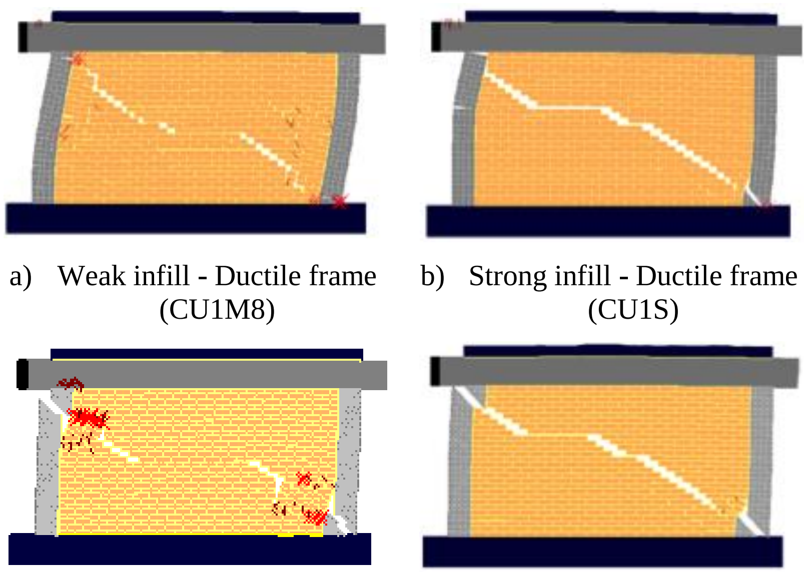

a) Weak infill - Ductile frame (CU1M8)

b) Strong infill - Ductile frame (CU1S)

c) Weak infill - Non-Ductile frame (P2Ro4)

d) Strong infill - Non-Ductile frame (CU1)

Fig. 4 – Types of failure mechanisms

The RC frame can exhibit either shear or flexure-dominated behavior depending on the infill properties and the relative shear to flexural capacity of the columns. When the infill is weak and does not resist the deformation of the frame, the interstory drift can be distributed within a larger portion of the column height. Hence, the shear demand is reduced and a flexural failure is more likely to develop as shown in Fig.4. Besides the strength of the infill, the shear resistance of the columns also affects the failure pattern.

Based on the observed failure mechanisms the infilled RC frames can be group in four cases:

Weak infill - Ductile frame

In the case of a weak infill with a ductile frame, sliding occurs in a number of bed joints along the height. At larger drifts the masonry panel crushes near the columns, where the struts develop, due to the concentration of high compressive stresses. The crushing of the masonry limits the forces applied on the columns which have enough shear capacity to avoid a shear failure. As a result, they deform flexurally in a ductile manner. This type of behavior can be observed either when hollow bricks are used to construct the infill or when the length of the infill is small, and thus the height-to-length aspect ratio large.

Weak infill - Non-Ductile frame

This case is the least common as in the event of a weak infill, the columns are more likely to avoid brittle shear failure. However, in case the RC framce is poorly detailed against shear, this mechanism can occur as illustrated in Fig. 4c. Similar to the case of a weak infill and a ductile frame, the infill cruches near the corners of the panel but shear cracks still develop at the RC columns leading to a brittle overall behavior of the structure.

Strong infill - Ductile frame

In the case of a strong infill with a ductile frame, the infill can carry large forces which are applied on the columns. The columns in this case accommodate the imposed drift within a short height due to the strong infill which restricts the deformation of the frame. Hence, the shear demand on the columns is large; however, the RC columns have enough shear capacity to accommodate this demand. This leads to large curvature locally and the formation of plastic hinges closely spaced along the column height. Eventually, the frames in this category may develop shear cracks in the columns at large drifts. However, these cracks do not have a noticeable effect on the ductile behavior of the frame.

Strong infill - Non-Ductile frame

Most of the older structures fall within this category [11] which is the most vulnerable one. This is because frames used to be detailed poorly for shear forces as those were typically underestimated or even ignored in the design. Moreover, the infills were typically constructed with multiple wythes of solid bricks which allowed them to develop large strut forces. The high infill strength leads to the development of few dominant diagonal shear-sliding cracks in the infill which eventually propagate through the poorly designed columns near the top of the windward and the bottom of the leeward column. Typically, tension develops in the windward column due to resist the overturning moment. Hence, this column develops a shear crack first, as the additional compression forces that develop in the leeward column increase its shear strength. Eventually, a shear cracks develops in this column as well, causing a significant drop of the load resistance which leads to a brittle failure.

4.2 Criteria for classification

The results of the parametric study have led to the development of classification criteria which are summarized at Table 3. Accordingly to the proposed criteria the masonry panel of an infilled reinforced concrete frame is first classified as weak or strong based on the ratio of stiffnesses between the infill and the columns. Once the infill is classified, the frame is characterized as brittle or ductile based on the ratio of the resistance to the development of a shear crack to the shear force required to develop two plastic hinges in the column. The two ratios, $\frac{K_{inf}}{K_c}$ and $\frac{V_n}{V_p}$ can be calculated using Equations (1) to (5).

$$K_{inf} = \frac{1}{\frac{1}{K_{inf,f}} + \frac{1}{K_{inf,s}}} \quad (1)$$

$$K_{\text{inf},f} = \frac{3E_m I_{\text{inf}}}{h_{\text{inf}}^3} \quad (2)$$

$$K_{inf,s} = \frac{A_{inf} G_m}{h_{inf}} \quad (3)$$

$$K_c = \frac{3E_c I_c}{h_{inf}^3} \quad (4)$$

$$V_p = \frac{2M_p}{h_p} \quad (5)$$

Table 3 - Classification of infilled reinforced concrete frames

Frame \ Infill	Weak	Strong
Ductile	$\frac{K_{inf}}{K_c} \leq 120$ $\frac{V_n}{V_p} > 1$	$\frac{K_{inf}}{K_c} > 120$ $\frac{V_n}{V_p} > 1$
Non-Ductile	$\frac{K_{inf}}{K_c} \leq 120$ $\frac{V_n}{V_p} \leq 1$	$\frac{K_{inf}}{K_c} > 120$ $\frac{V_n}{V_p} \leq 1$

where $K_{\text{inf},f}$ is the infill flexural stiffness, $K_{\text{inf},s}$ is the infill shear stiffness, K_c is the column flexural stiffness, V_p is column shear force that can lead to the development of plastic hinges over the column at a distance h_p, L_{inf} is the length of the infill panel, t_{inf} is the thickness of infill panel, A_{inf} is the horizontal cross-sectional area of an infill panel ($t_{inf} \times L_{inf}$), E_c is the modulus of elasticity of concrete, E_m is the modulus of elasticity of masonry, G_m is the shear modulus of masonry, h_{inf} is the height of the infill panel, I_{inf} is the moment of inertia of infill panel, I_c is the moment of inertia of a column, M_p is the plastic moment capacity of the RC column, and V_n is the column shear strength accounting for the shear resistance of concrete and transverse reinforcement.

These quantities can be calculated if the geometry and basic material properties are known or can be assumed. Typically, it cannot be known *a priori* where the plastic hinges in the column will develop. Hence, h_p may not be known. The analysis of the parametric study results indicates that, h_p can be assumed equal to the infill height divided by α, where α is 2 in case of a weak infill, and 2.5 in case of a strong infill when the height to length ratio is smaller than 1. When this ratio is larger than 1, α can be assumed to be 1, i.e. in this case h_p is taken to be equal to the infill height.

5. Validation

The proposed methodology has been applied to all infilled frames considered in this study. The classification of all frames is illustrated in Fig.5 and it matches the observed failure patterns which are not presented here for conciseness. Fig.5 also presents the classification of the 11 infilled frames tested by Mehrabi et al. [6]. The design details of these frames are summarized in Table 4, and their failure patterns and force-vs.-displacement curves are shown in Fig.6. As it can be seen in the figure, all cases have been classified correctly by the proposed criteria.

In summary, most speciments with solid bricks are classified as strong infills, while the structures with hollow bricks are classified as weak infills. All specimens classified as ductile frames develop flexural cracks in the RC columns, while the specimens classified as non-ductile are dominated by shear failures. An exception to this is Specimen 7 which is categorized as weak infill despite having solid brick infill. However, the failure of this specimen involved damage spread along the column height indicating that the RC frame could deform without considerable restraints imposed by the infill. This increased deformability was a result of larger columns which were stronger with respect to the infill compared to the other specimens.

Table 4 - Properties of specimens tested by Mehrabi et al. [6]

Specimen	Brick	f'c	f'm	Column dimensions		Infill dimensions		Ratio Column Reinforcing	Stirrup Spacing	Axial Load
				b	d	lw	hw			
		[MPa]	[MPa]	[cm]	[cm]	[cm]	[cm]	[%]	[cm]	[kN]
specimen2*	hollow brick	31	10	18	18	213	164	3.21%	6.4	294
specimen3*	solid brick	31	15	18	18	213	164	3.21%	6.4	294
specimen4	hollow brick	27	11	18	18	213	164	3.21%	6.4	294
specimen5	solid brick	21	14	18	18	213	164	3.21%	6.4	294
specimen6	hollow brick	26	10	20	20	213	164	3.83%	3.8	294
specimen7	solid brick	33	14	20	20	213	164	3.83%	3.8	294
specimen8*	hollow brick	27	10	18	18	213	164	3.21%	6.4	294
specimen9*	solid brick	27	14	18	18	213	164	3.21%	6.4	294
specimen10	hollow brick	27	11	18	18	295	164	3.21%	6.4	294
specimen11	solid brick	26	11	18	18	295	164	3.21%	6.4	294
specimen12*	solid brick	27	14	18	18	295	164	3.21%	6.4	440

* Repaired specimen

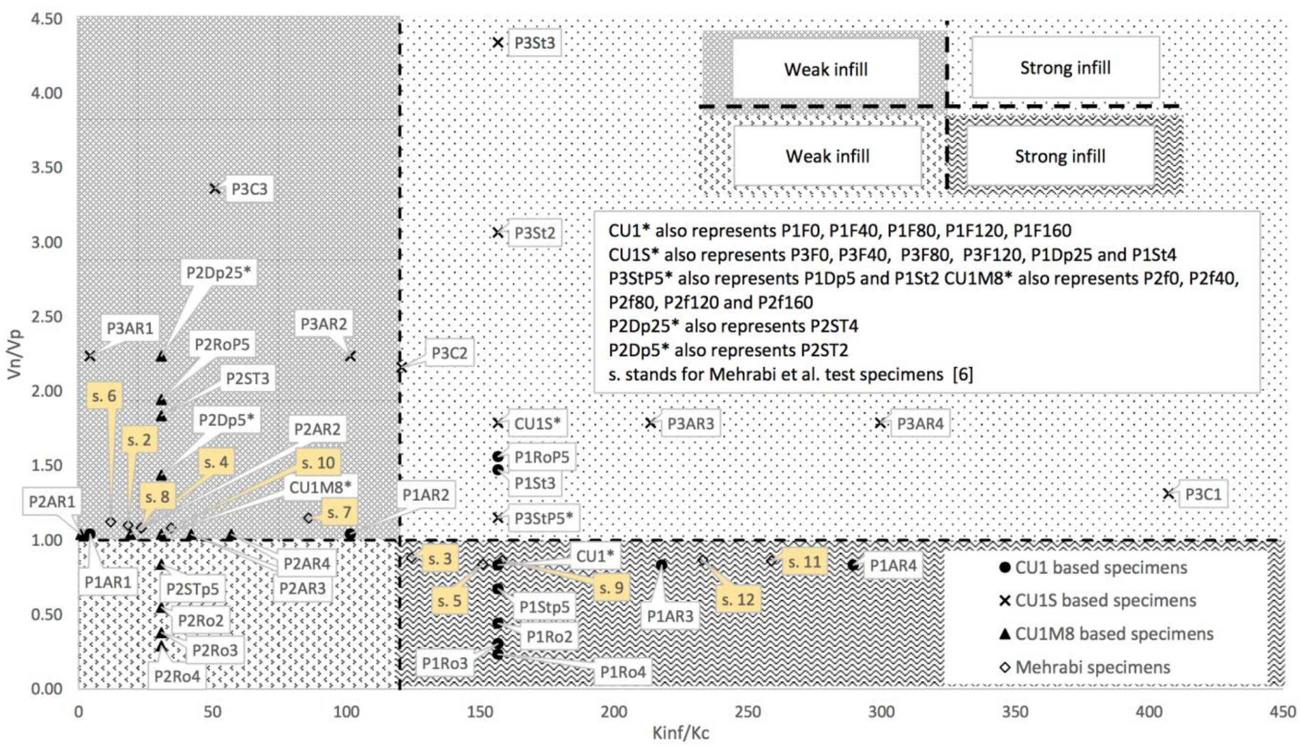

Fig. 5 – Calssification of infilled frames considered in this study.

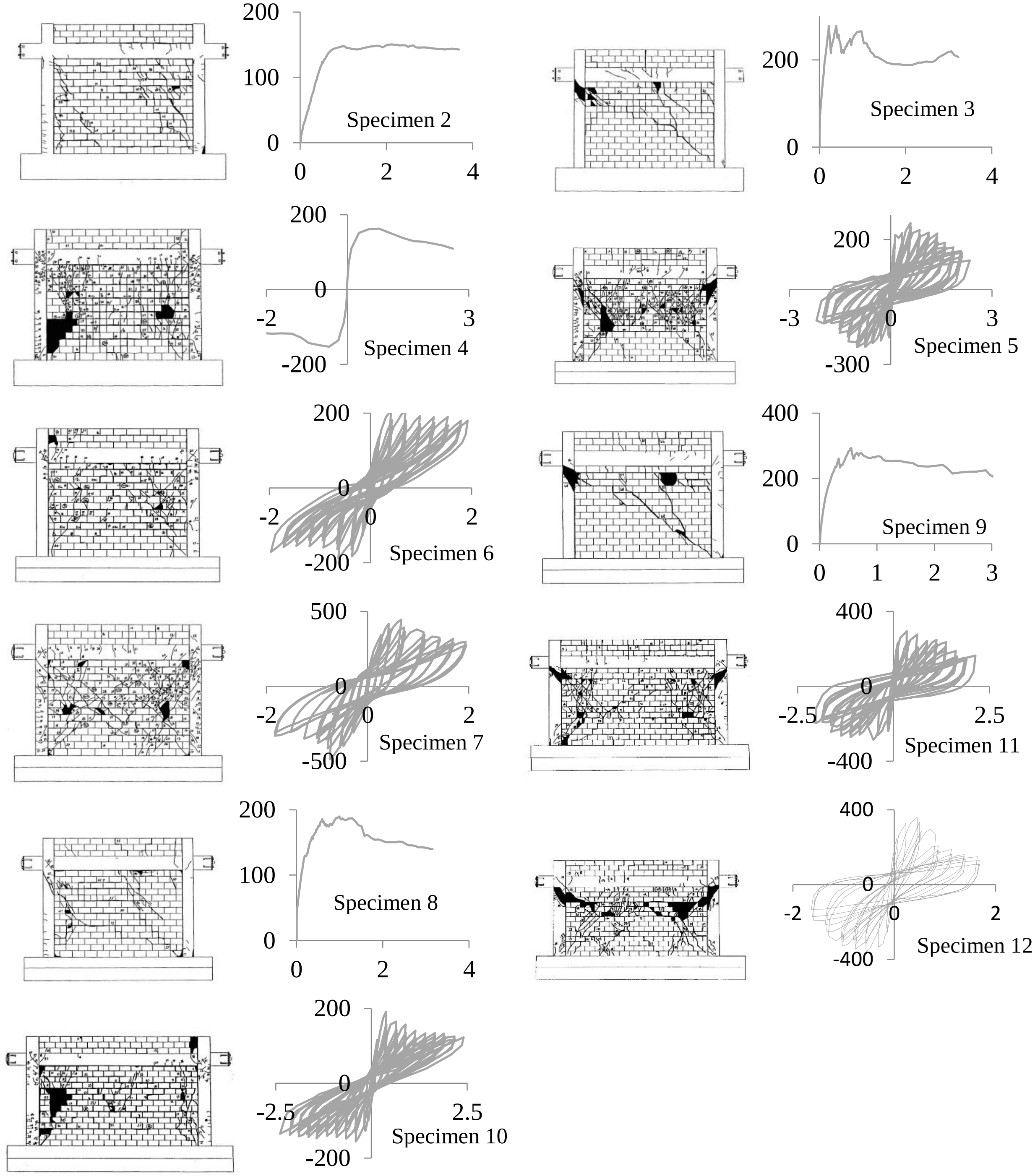

a) Weak infill - Ductile frame Cases b) Strong infill - Non-Ductile frame

Fig. 6 – Mehrabi based specimen validation (drifts are express in % and forces in kN) [6]

6. Conclusions

This paper summarizes the results of an extensive parametric study using validated FE analysis which investigates the performance of single-bay, single-story RC frames with solid masonry infills. The study of the failure patterns and force-vs.-displacement curves indicates that the behavior can be classified in four categories, each of which can be associated with a distinct failure pattern. The infilled frames can be accurately classified in the appropriate category based on the ratio of the infill to column stiffness and the ratio of the shear to flexural strength of the columns. The proposed framework is validated with the structures considered in the parametric study, as well as infilled RC frames tested in the laboratory. The comparison of the predicted and actual failure mechanisms indicates that the framework can correctly classify all frames and therefore predict their failure pattern. The ability to *a priori* predict the failure patter is critical for the prediction of the strength of these frames which is one of the most significant challenges for practicing engineers.

7. Acknowledgements

The first author of the paper is grateful for the financial support provided by University at Buffalo and BEC.AR Argentine Presidential Fellowship in Science & Technology throughout her graduate studies. The assistance of Austin Reese and Laura Pavone is also acknowledged. However, the opinions expressed in this paper are those of the authors and do not necessarily represent those of the sponsors or the collaborators.

8. References

[1] ASCE/SEI 41-06. (2006): Seismic Rehabilitation of existing buildings. *ASCE*, New York.

[2] ASCE/SEI 41-13. (2013): Seismic Evaluation and Retrofit of Existing Buildings. *ASCE*, Reston, Virginia.

[3] Stafford-Smith, B. and Carter, C. (1969): A Method for the Analysis of Infilled Frames. *Proceedings of the Institution of Civil Engineers*, 44, 31-48.

[4] Mainstone, R. (1971): On the Stiffnesses and Strengths of Infilled Frames. *Proceedings of the Institution of Civil Engineers*, Supplement IV, 57-90.

[5] Wood, R.H. (1978): Plasticity, Composite Action and Collapse Design of Unreinforced Shear Wall Panels in Frames. *Proceedings of the Institution of Civil Engineers*, Part 2, 65, 381-411.

[6] Mehrabi, A.B., P.B. Shing, M.P. Schuller, and J.L. Noland (1994): Performance of masonry-infilled R/C frames under in-plane lateral loads. *Report No. CU/SR-94/6*, University of Colorado at Boulder.

[7] Mehrabi, A.B. and P. B. Shing (1997): Finite element modeling of masonry-infilled RC frames. *J. Struct. Eng.*, ASCE, Vol. 123(5), 604-613.

[8] Al-Chaar, G., Mehrabi, A. B., and Manzouri, T. (2008): Finite element interface modeling and experimental verification of masonry-infilled R/C frames. *The Masonry Society Journal*, Vo. 26(1), 47-65.

[9] Stavridis, A. and Shing, P.B. (2010): Finite-Element Modeling of Nonlinear Behavior of Masonry-Infilled RC Frames, *Journal of Structural Engineering*, Vol. 136, No. 3, 285–296.

[10] Koutromanos, I., Stavridis, A., Shing, P.B., and Willam, K. (2011): Numerical modeling of masonry-infilled RC frames subjected to seismic loads. *Computers and Structures*, Vo. 89, pp. 1026-1037.

[11] Stavridis, A. (2009): Analytical and Experimental Study of Seismic Performance of Reinforced Concrete Frames Infilled with Masonry Walls, *Ph.D. Dissertation*, University of California at San Diego, La Jolla, CA.

[12] Blackard, B., K. Willam, and S. Mettupulayam (2009): Experimental observations of masonry infilled RC frames with openings. *ACI Special Publication SP-265*, American Concrete Institute, Farmington Hills, MI.

[13] Reese, A. (2013): Simplified Analysis of Masonry-Inifilled RC Frames Subject to Lateral Loading. *Master's Thesis*, University of Texas at Arlington, Arlington TX.

[14] Reese, A. and Stavridis, A. (2014): A simplified method for the estimation of the seismic resistance of RC frames with weak infill panels, *Tenth U.S. National Conference on Earthquake Engineering*, Alaska, USA